SPINEL CRYSTAL DISTRIBUTION AND SETTLING IN A HIGH-LEVEL WASTE MELTER WORKING AS A PERFECT MIXER

PART 2. RESULTS OF CALCULATIONS

MILOŠ JIŘIČKA, LUBOMÍR NĚMEC

Laboratory of Inorganic Materials
Joint workplace of the Institute of Inorganic Chemistry of the Academy of Sciences of the Czech Republic and the Institute of Chemical Technology, Prague, Technická 5, 166 28 Prague, Czech Republic

E-mail: nemecl@vscht.cz

Submitted May 20, 2002; accepted August 2, 2002

Keywords: Particle settling, High-level waste, Perfect mixer

The developed models of crystal distribution and settling in a vitrification space working either as the perfect mixer or space with the piston flow were applied to compare their results with the numerical mathematical model of the real vitrification space. In this study, the influence of temperature, initial spinel crystal size and concentration in the batch, glass liquidus temperature and melter pull rate on the thickness of the crystal layer were examined. The results demonstrated the decisive role of the initial crystal size and character of the melt flow on the crystal settling rate and crystal layer growth. The comparison of results of both models has shown that the real vitrification space behaves similarly as the combination of the short-term piston flow and the subsequent perfect mixer.

INTRODUCTION

The behavior of glass melting and vitrification spaces may be often expressed by means of a combination of perfect mixing and piston flow provided results of melter transition characteristics are at disposal. The results can also serve as a base for simplified models of solid particle or bubble distribution if their settling or rising velocities are sufficiently low. Application of the mentioned models as qualitative tools for evaluation of melting or vitrification abilities of the facility is attractive owing to their very short calculation times and a lower need of input data. At present, the appropriate theoretical approach to the combined glass flow is not at disposal yet, however, authors of this work have derived a distribution model of spinel crystals interacting with the melt and settling in the HLW melter when the space is perfectly mixed or with the piston flow inside [1]. As the previous works in this field have shown [2-5], the slowly dissolving Fe, Cr and Ni spinel crystals in the melt settle at temperatures above liquidus on the vitrification melter bottom and its oblique sides and form a growing crystal layer of high viscosity (sludge layer). The thick layers are blocking especially the output channels and reduce the lifetime of the facility. The 3D mathematical modelling of this phenomenon [6,7] was able to provide a better understanding of the mechanism of crystal interactions and settling and thus opened the way to intensification of the process. The results also showed that the vitrification space is intensively mixed by free convection and consequently, the space behaves as a perfect mixer as for the crystal distribution inside the space. These results justify the tentative application of the already mentioned simplified model of the perfect mixer in a study of vitrification characteristics of the HLW melter. A considerable shortening of calculations can be expected, and more suitable input data from this model may be gained for application in the numerical mathematical model.

The goal of this work is to compare the results of the numerical mathematical model [7] with corresponding values coming out from the model of the perfect mixer, as well as from the piston flow model. In the subsequent part of the work, the results of the parametric study will be presented, elucidating the influence of melt temperature, initial spinel crystal concentration and size, melt liquidus temperature, mass transfer coefficient of crystal dissolution and melter pull rate on the thickness of the crystal sludge layer in the melter.

THEORETICAL

The steady concentration of crystals in the perfectly mixed vitrification space, provided the crystal input, output, dissolution and settling are considered, is given by [1]:

$$C_\infty = \frac{\dot{V}C_{in}}{\frac{0.205g\Delta\rho}{\eta}\left(a_o + \dot{a}\overline{\tau}_{Age}\right)^2 S + \dot{V} - \frac{3\dot{a}V}{a_o + \dot{a}\overline{\tau}_{Age}}} \quad (1)$$

where $\dot{V}$ is the volume output from the space, C_{in} is the crystal input concentration, $\Delta\rho$ is the density difference of crystals and melt, η is the melt viscosity, a_0 the initial crystal size, $\dot{a}$ the rate of crystal dissolution in the steady state, $\overline{\tau}_{Age}$ is the average age of all crystals and S is the settling surface.

In equation (1), the crystal nucleation is not taken into account as the input crystal concentrations, as well as average vitrification temperature, are sufficiently high.

The thickness of the crystal layer in time τ under equivalent conditions is described by:

$$h_{cr}(\tau) = \frac{0.205g\Delta\rho}{\eta C_{layer}}\left(a_0 + \dot{a}\overline{\tau}_{Age}\right)^2 C_\infty \quad (2)$$

The expressions for the value of $\overline{\tau}_{Age}$ is given by equation (30) in [1].

Under conditions of the piston flow, the average crystal concentrations in the melter space are given by equations [1]:

$$\frac{dC}{d\tau} = \frac{C_{in}\dot{V}}{Va_0^3}a^3(\tau)d\tau \quad (3)$$

and:

$$\frac{da}{d\tau} = k_H\left[C_0 - \frac{C_{in}}{a_0^3\rho_s}a^3(\tau)\right] \quad (4)$$

Equations (1-4), together with equations (30) and (34-36) in [1], were applied to compare the results of numerical mathematical model with the model of the perfect mixer, as well as the piston flow, and to examine the influence of parameters on the crystal settling in the vitrification space.

RESULTS OF CALCULATIONS

The results of the real HLW melter filling by a new glass with dissolving crystals obtained in [7] by the numerical mathematical model were used to compare the melter behavior with the models of perfect mixing and piston flow. The comparison for crystals of constant size (simulating the filling by a new glass melt) is plotted in figure 1. Equations (31) and (35) from [1], as well as data presented in table 1 were used for calculation of the reference case. As is obvious, the behavior of the real melter is apparently different from the piston flow model but approaches well to the perfect mixer. When calculating the same concentration developments for crystals dissolving in the melt according to data in table 1 and equations (34-36) in [1], as well as (3-4) in this work, results presented in figure 2 are acquired. The mathematical model and the model of perfect mixer exhibit distinctly higher average concentrations of crystals in the melter when compared with the piston flow model. The reason of this difference lies most probably in higher local concentrations of crystals in the non-stirred piston flow model which enhance the crystal dissolution. The numerical mathematical model and the perfect mixer model differ within 10% in the stationary state, the consent between both solutions is better in the initial period of melter filling by crystals. Both figures show that the behavior of the real HLW melter approaches sufficiently to the perfect mixer.

The presented examples of behavior justify the application of the perfect mixer model for the parametric study of the HLW melter. To calculate the influence of parameters on the spinel settling in the melter, the steady concentration of spinel crystals was calculated using equation (1) and Hixon-Crowell equation (see equation (40) in [1]). The total layer thickness was calculated from equation (2) in this work, crystal nucleation was not considered. Besides the mentioned values, the value of $\overline{a}_{CC}^2$ (the square of average size of crystals coming from the cold cap in the melter) and the steady crystal concentration in the melter, C_∞, both contributing to the crystal layer growth, were plotted in appropriate pictures. The impact of the melt temperature (see figu-

Table 1. Input values for the reference case.

Temperature (average)	1104	(°C)	[7]
Liquidus temperature	1078	(°C)	[8]
Glass density	2437	(kg/m^3)	ρ_s=2722.7-0.2077*T, [7]
Spinel density	5140	(kg/m^3)	[7]
Initial concentration of spinel	110	(kg/m^3)	[7]
Concentration of spinel in the sludge layer	822	(kg/m^3)	[4]
Initial size of crystals	1×10^{-6}	(m)	[7]
Mass transfer coefficient	2.51×10^{-9}	(m/s)	k_H=0.1777*exp(-24891/T), [2]
Settling surface	1.28	(m^2)	[7]
Melting space volume	1	(m^3)	[7]
Equilibrium concentration of spinel	-3.21×10^{-3}	(m^3/m^3)	C0=0.004334*(1-exp(5110.7*(1/T-1/T_L))), [9]
Pull rate	5.13×10^{-6}	(m^3/s)	[7]
Glass viscosity	7.55	(Pa s)	[7]

T - temperature in Kelvins
T_L - liquidus temperature (K)

re 3), initial concentration of spinel crystals (figure 4), initial size of spinel crystals (figure 5), mass transfer coefficient (figure 6), glass liquidus temperature (figure 7) and melter pull rate figure (8), were investigated in these calculations. To compare the behavior of the perfect mixer with the numerical 3D model of the real HLW melter, the values of h_{cr} calculated by the 3D model are presented in appropriate figures too [7].

DISCUSSION

The dependence of h_{cr} on temperature exhibits the maximum at temperatures about 120 °C below liquidus temperature (see figure 3). The crystals dissolve in the entire temperature interval ($\dot{a}$ = 0 at 878 °C). At higher temperatures, the thickness of the layer decreases owing to increasing crystal dissolution rate. This fact is expressed by decreasing values of both C_∞ and $\bar{a}_{CC}$ with growing temperature. The mentioned influence exceeds the enhancing impact of decreasing viscosity on the crystal settling rate. The lower temperature region is characterized by slowing down the crystal dissolution rate and by the exponential increase of viscosity. The decisive role plays here the decreasing rate of crystal settling due to growing viscosity, consequently the crystal layer thickness decreases too. The reference value of the crystal layer thickness in the reference case (1104 °C) was 80.7 μm for the perfect mixer and 37 μm for the mathematical model, thus being about twice higher than exhibits the model of real melter. The corresponding values for numerical model of the real melter at temperatures 1074 °C and 1094 °C were 50 μm and 40 μm, respectively, thus exhibiting the lower slope than the perfect mixer.

The steady increase of the value of crystal layer thickness with the initial spinel crystal concentration in the batch is obvious from figure 4. This is brought about by the growing value of steady crystal concentration in the melter; the crystal concentration growth outweighs the fact that the value of $\bar{a}_{CC}$ goes down, i.e. the dissolution rate of crystals grows. The values of h_{cr} calculated from the 3D numerical model are about half of the value obtained by the model of perfect mixer (see points in figure 4).

The impact of the initial crystal size on the layer thickness appears most significant. With the growing crystal size the overall crystal surface decreases, i.e. the dissolution rate and consequently, both C_∞ and $\bar{a}_{CC}$ grow. The dependence between the layer thickness and the initial crystal size has an expected parabolic shape as is presented in figure 5. The crystal layer thickness can be dangerous for the melter operation at the values of a crystal size 10 μm and more. Experiments show the presence of coarser crystals in a melted batch [10], that is why the control of crystal nucleation in the early stage of melting is technologically important. The values of h_{cr} obtained by the 3D mathematical model amounted to 338 μm and 1802 μm at initial sizes 2.5 and 5 μm, respectively, and exhibit 2-4 times lower values when compared with the model of the perfect mixer.

The dependence between the layer thickness and the value of mass transfer coefficient has an expected falling character due to the decreasing rate of crystal dissolution in the melt as figure 6 shows. Both the value of C_∞ and $\bar{a}_{CC}$ go down with growing mass transfer coefficient. The presented results have only an indicative value as the mass transfer coefficient is in an intricate way dependent on batch composition and process conditions. Similar indicative value can be attributed to the dependence between the crystal layer thickness and liquidus temperature of the melt, presented in figure 7. The value of h_{cr} steeply increases as the liquidus temperature of the melt rises, that is demonstrated by growing C_∞ and $\bar{a}_{CC}$. The values of the liquidus temperature are as in the previous case dependent on the melt composition, especially on the content of spinel forming components. The composition changes are linked with changing glass properties and crystal behavior in the melt. The values of h_{cr} acquired by the 3D mathematical model are as well 2-3 times lower than the perfect mixer model exhibits.

The maximum allowed pull rate of the HLW melter is a primary technological parameter. As is seen from figure 8, an almost linear increase of the crystal layer thickness with the melter pull rate can be expected. The decreasing average residence time of the melt in the melter with an increasing pull rate is demonstrated by the increase in both C_∞ and $\bar{a}_{CC}$. Nevertheless, the slope of this dependence allows a higher pull rate than the reference value 5.13×10^{-6} m^3/s without a dramatic increase in the layer thickness.

As is apparent from the presented comparison between both models, the values of the 3D mathematical model are 2-3 times lower than these coming from the model of the perfect mixer. The difference between both models suggests that the real melter does not behave completely as the perfect mixer. In the real melting space, the entering glass melt with crystals flows from the cold cap (batch blanket) to the bottom and outflow channels; during this relatively short time period before mixing by natural convection, the character of melt flow approaches the piston flow. The character of melt flow in the entire vitrification space could be therefore expressed as a combination of the piston flow and the subsequent perfect mixer. A trial has been undertaken to evaluate how the piston flow shares in the resulting crystal concentration in the melter and the thickness of crystal layer. Equations (3-4) were applied to calculate the values of local crystal concentration and crystal size after passing through a piston flow period. The

final values were used for calculations of perfect mixing in the remaining part of the melter by applying equations (1-2). The average crystal concentration in the entire melter and the thickness of the crystal layer were then calculated and are plotted in figure 9. The increasing proportion of the prior piston flow decreases sharply the crystal concentration in the perfectly mixed part of the melter and the crystal layer is therefore thin. The presented results show that the thickness of crystal layer calculated by the 3D model (37 μm) corresponds to the combination of the piston flow and the perfect mixer where the piston flow occupies about 2500s from the entire residence time of the melt in the space, amounting to 1.95×10^5s. Despite this small proportion of the piston flow, its existence in the upper parts of the melter can significantly suppress the layer growth. Therefore, the proper melt flow distribution in the melter could have favourable effect on the crystal settling.

CONCLUSION

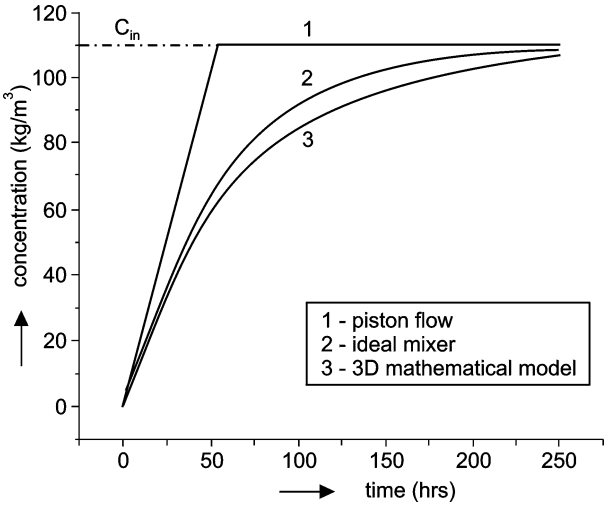

Figure 1. The melter filling by crystals of constant size (expresses melter filling by a new glass, reference case with data from table 1).

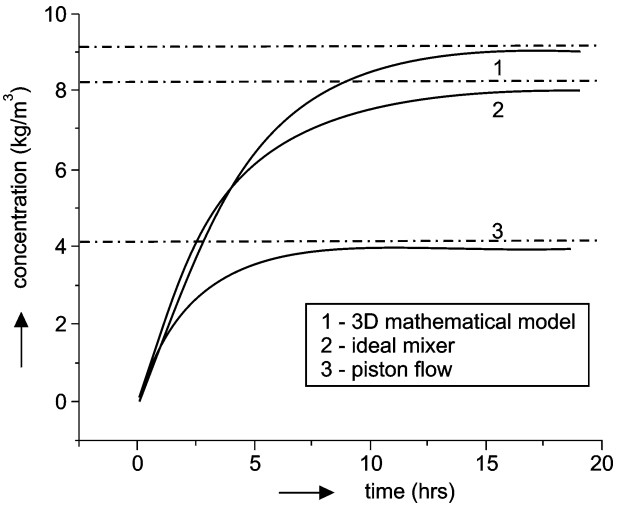

Figure 2. The melter filling by dissolving crystals - reference case, see table 1.

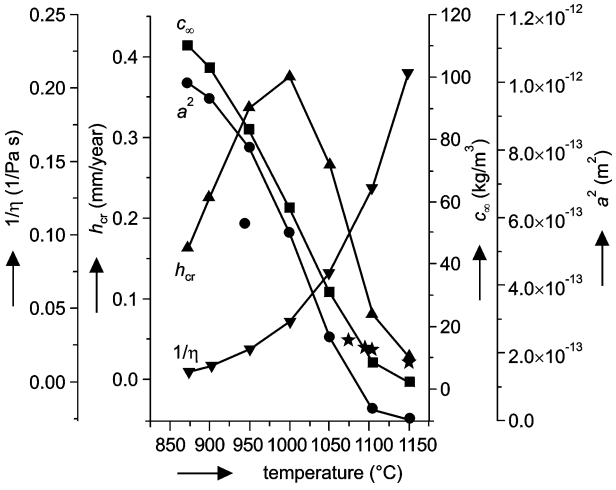

Figure 3. The impact of the melt temperature on the layer thickness of settled spinel crystals in the perfectly mixed space. ▲ - the crystal layer thickness after one year campaign; ■ - the steady spinel crystal concentration in the melter; ● - the square of the average size of crystals in the melter; ▼ - the reciprocal value of the dynamic viscosity; ★ - the layer thickness from the 3D numerical mathematical model.

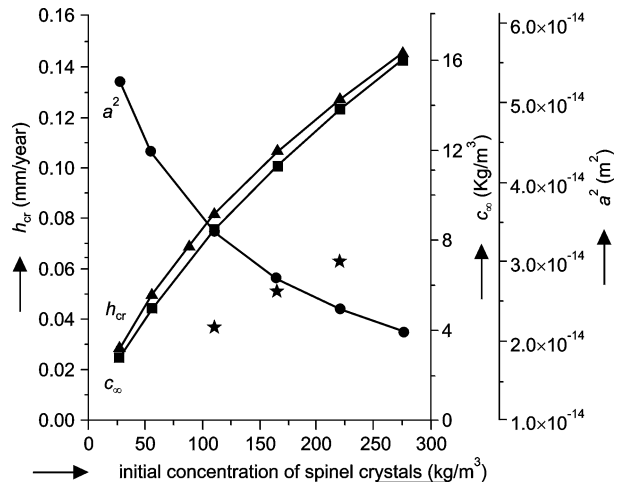

Figure 4. The impact of the initial concentration of spinel crystals on the layer thickness of settled crystals in the perfectly mixed space. ▲ - the crystal layer thickness after one year campaign; ■ - the steady spinel crystal concentration in the melter; ● - the square of the average size of crystals in the melter; ★ - the layer thickness from the 3D numerical mathematical model.

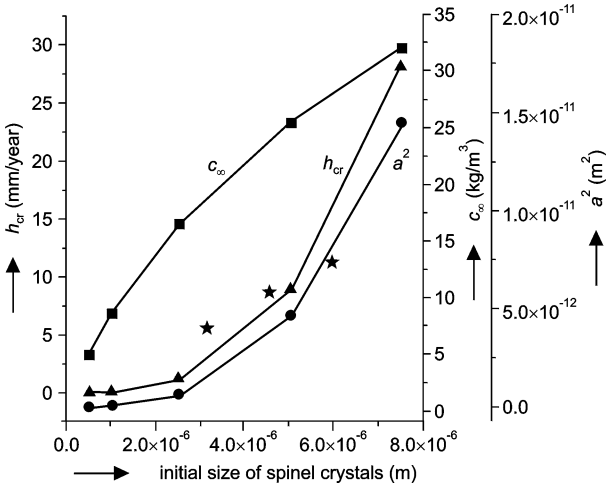

Figure 5. The impact of the initial size of spinel crystals on the layer thickness of settled crystals in the perfectly mixed space. ▲ - the crystal layer thickness after one year campaign; ■ - the steady spinel crystal concentration in the melter; ● - the square of the average size of crystals in the melter; ★ - the layer thickness from the 3D numerical mathematical model.

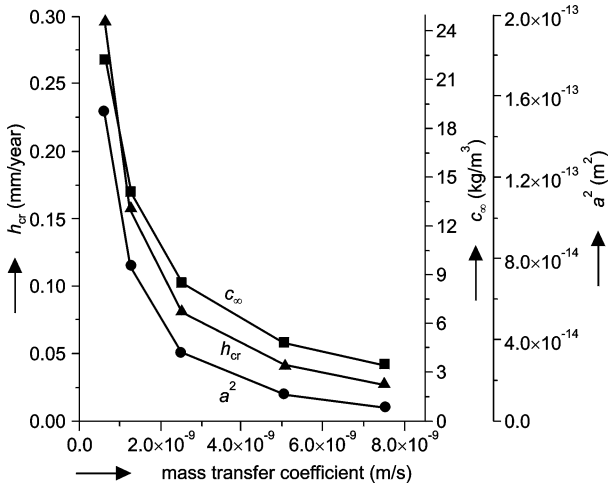

Figure 6. The impact of the value of the mass transfer coefficient, k_H, on the layer thickness of settled spinel crystals in the perfectly mixed space. ▲ - the crystal layer thickness after one year campaign; ■ - the steady spinel crystal concentration in the melter; ● - the square of the average size of crystals in the melter.

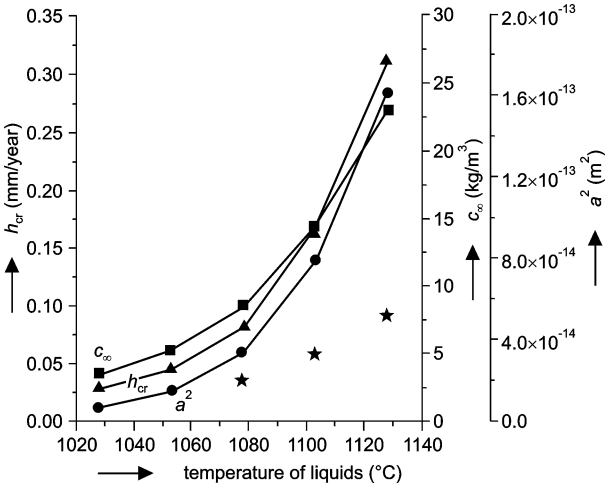

Figure 7. The impact of the liquidus temperature of glass on the layer thickness of settled spinel crystals in the perfectly mixed space. ▲ - the crystal layer thickness after one year campaign; ■ - the steady spinel crystal concentration in the melter; ● - the square of the average size of crystals in the melter; ★ - - the layer thickness from the 3D numerical mathematical model.

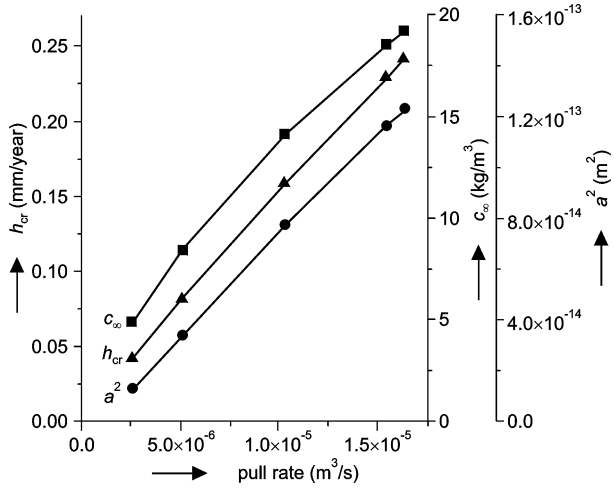

Figure 8. The impact of the pull rate of the melter on the layer thickness of settled spinel crystals in the perfectly mixed space. ▲ - the crystal layer thickness after one year campaign; ■ - the steady spinel crystal concentration in the melter; ● - the square of the average size of crystals in the melter.

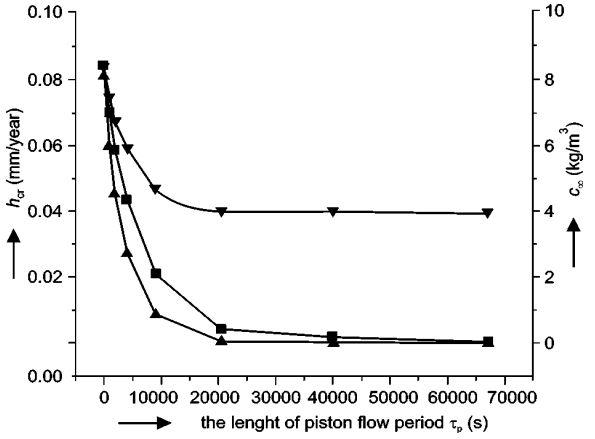

Figure 9. The dependence of the crystal layer thickness and the average crystal concentrations in the entire melter space on the time the glass melt underwent piston flow. ▼ - the average crystal concentration in the entire melter space; ■ - the average crystal concentration in the perfectly mixed part of the melting space; ▲ - the crystal layer thickness after one year campaign.

The mathematical modeling of melting spaces is a complicated and laborious procedure demanding numerous data about a melt, melting space and melting kinetics. That is why any simplifying procedure giving acceptable results or true tendencies are welcome. The simplifying procedure requiring only negligible calculation times and limited data makes it possible to realize instantly extended parametric studies. Their results can be also used as initial conditions for complete mathematical models to shorten considerably the numerical calculations. The analysis of glass flow in the HLW melter showed that the melter behavior can be approximately replaced by melting in a perfect mixer. This behavior is due to relatively rapid melt rotation cells present in the actual melter. In consent with the results of the complete model, the calculated crystal layers in the perfect mixer are thin with the exception of coarse crystals. The comparison of the 3D mathematical model and the perfect mixer model has shown that the 3D mathematical model provides 2-3 times lower values of crystal layer thicknesses in most compared cases. This difference is due to a short-term participation of the piston flow in the initial vitrification period. The greater was the participation of the piston flow, the thinner were the layers of dissolving crystals. Therefore, the establishing the piston flow in the initial vitrification period has a favourable technological consequence and should be studied by numerical mathematical models. Thus the application of the combined piston flow and the perfect mixer models revealed the character of the melt flow and could help in establishing optimum technological parameters.

Acknowledgement

This work was supplied with the subvention by Grant Agency of AS CR, Project No. S4032103.

References

1. Němec L., Jiřička M.: Ceramics-Silikáty *46*, 81 (2002).
2. Hrma P., Alton J.: Proceedings of the ICEM´01, The 8th International Conference on Radioactive Waste Management and Environmental Remediation, Bruges, Belgium 2001 (CD ROM).
3. Kloužek J., Alton J., Plaisted T.J., Hrma P.: Ceram.Trans. *119*, 301 (2001).
4. Míka M., Hrma P., Schweiger M.J.: Ceramics-Silikáty *44*, 86 (2000).
5. Jiřička M., Hrma P.: Ceramics-Silikáty *46*, 1 (2002).
6. Matyáš J., Němec L., Kloužek J., Trochta M.: Proceedings of the ICEM´01, The 8th International Conference on Radioactive Waste Management and Environmental Remediation, Bruges, Belgium 2001 (CD ROM).
7. Matyáš J., Němec L.: Submitted for publication in Ceram.Trans.
8. Hrma P., Vienna J.D., Crum J.V., Piepel G.F., Míka M.: Mat.Res.Soc.Proc. *608*, 671 (2000).
9. Wilson B.K., Plaisted T.J., Alton J., Hrma P.: Submitted for publication in J.Mat.Sci. (2001).
10. Kloužek J., Cihlářová K.: Private communication.

KONCENTRACE SPINELOVÝCH KRYSTALŮ A JEJICH USAZOVÁNÍ V TAVICÍM ZAŘÍZENÍ PRO VITRIFIKACI VYSOCE RADIOAKTIVNÍCH ODPADŮ

ČÁST 2. VÝSLEDKY VÝPOČTŮ

MILOŠ JIŘIČKA, LUBOMÍR NĚMEC

Laboratoř anorganických materiálů
Společné pracoviště Ústavu anorganické chemie
Akademie věd České republiky
a Vysoké školy chemicko-technologické v Praze
Technická 5, 166 28 Praha

Modely ideálního mísiče a pístového toku popisující rozložení krystalů v tavicím prostoru pro vitrifikaci vysoce radioaktivních odpadů byly použity pro porovnání jejich výsledků s rozložením krystalů a tloušťkou vrstvy usazených krystalů získaných pomocí numerického matematického modelu reálného vitrifikačního prostoru. V předložené studii byl zkoumán vliv počáteční koncentrace a rozměrů krystalů spinelu, teploty i teploty liquidus taveniny a výkonu prostoru na tloušťku vrstvy krystalů usazených na dně prostoru. Výsledky studie ukázaly rozhodující vliv počáteční velikosti krystalů a charakteru proudění na tvorbu vrstvy. Porovnání výsledků obou modelů ukázalo, že chování reálného vitrifikačního prostoru může být vyjádřeno pomocí sériové kombinace pístového toku a ideálního mísiče s velmi krátkým působením pístového toku.